THE JOURNAL OF PHYSICAL CHEMISTRY A
A JOURNAL OF THE AMERICAN CHEMICAL SOCIETY

pubs.acs.org/JPCA

Article

# Computational Insights into Tunable Reversible Network Materials: Accelerated ReaxFF Kinetics of Furan-Maleimide Diels–Alder Reactions for Self-Healing and Recyclability

L. Vermeersch, T. Wang, N. Van den Brande, F. De Vleeschouwer, and A. C. T. van Duin*

Cite This: *J. Phys. Chem. A* 2024, 128, 10431–10439

Read Online

ACCESS | Metrics & More | Article Recommendations | Supporting Information

**ABSTRACT:** In this study, ReaxFF molecular dynamics simulations were benchmarked and used to study the relative kinetics of the retro Diels–Alder reaction between furan and *N*-methylmaleimide. This reaction is very important for the creation of polymer networks with self-healing and recyclable properties, since they can be used as reversible linkers in the network. So far, the reversible Diels–Alder reaction has not yet been studied by using reactive molecular dynamics simulations. This work is, thus, the first step in simulating a covalent adaptable network (CAN) using Diels–Alder reactions as reversible linkers. For both *endo* and *exo*, the bond breaking in 40 product molecules was simulated using the bond boost method and the *endo*/*exo* ratio was evaluated. This ratio was benchmarked against density functional theory (DFT) and experimental results for a changing set of bond boost parameters. Given their importance to understand how the CAN performs, the effect of the addition of a polymer backbone and the effect of temperature were successfully simulated using our newly parametrized reactive force field.

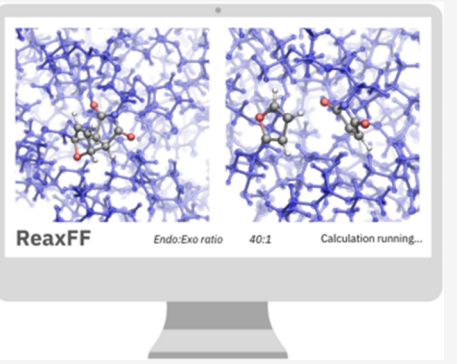




## INTRODUCTION

Current environmental and resource issues require us to rethink the way we create, use, and reuse materials. At this moment, no less than 25% of all polymeric materials in the EU end up in landfill, indicating the great challenges and opportunities for the polymer sector.[1] Covalent Adaptable Networks (CANs) can help us transition to a new era for materials scientists, where products based on polymers have an increased longevity and reuse is the norm.[2]

Reversible network materials are polymer networks that use reversible covalent bonds to cross-link the polymer chains.[3−5] Upon damage or heating the materials, these covalent bonds are preferentially broken and can be restored using a heat treatment. CANs can therefore "self-heal" and might combine the benefits of network polymers, with increased strength and longevity, with recyclability comparable to that of thermoplasts.[6]

A commonly used reaction for the creation of these CANs is the Diels–Alder (DA) reaction.[7,] The relatively low barrier ensures preferential breaking, and no side products are observed at temperatures where the CANs would be used (<130 °C).[4] Diels–Alder reactions are very versatile, and hundreds of different combinations of dienes and dienophiles could be used in these systems. Several of them were already used in self-healing networks, such as maleimide with furan and maleic acid with fulvene.[9,10] CANs based on furan-maleimide reactions have already shown their potential for self-healing materials and were thoroughly studied regarding their kinetics and thermodynamics by Mangialetto and Cuvellier et al.[11−15] The CANs based on the furan-maleimide reaction were already tuned by varying the stoichiometry of the mixtures, polymer chain length and curing methods.[2,9,16−18]

To understand how such a network is formed and how the resulting self-healing works, *in silico* modeling can complement the experimental findings. Importantly, accurate modeling involves the scrutiny of both kinetic and thermodynamic properties of these systems. Density functional theory (DFT) has been shown to be a useful quantum-mechanical method to study the DA reactivity through the computation of full reaction paths, which allow to determine forward and retro reaction barriers, reaction energies, and product stabilities using a relatively low computational demand. However, the model systems used in these quantum-mechanical calculations are often limited in size and therefore do not consider the full effect of the surrounding polymer network, which includes secondary interactions, chain mobility, plausible orientation of the DA components and reaction center accessibility. This, in turn, influences the observed experimental kinetics and thermodynamics as it might largely affect the stereoselectivity (*endo* vs *exo* diastereomers).

**Received:** August 26, 2024
**Revised:** October 15, 2024
**Accepted:** November 6, 2024
**Published:** November 20, 2024





https://doi.org/10.1021/acs.jpca.4c05470
*J. Phys. Chem. A* 2024, 128, 10431–10439

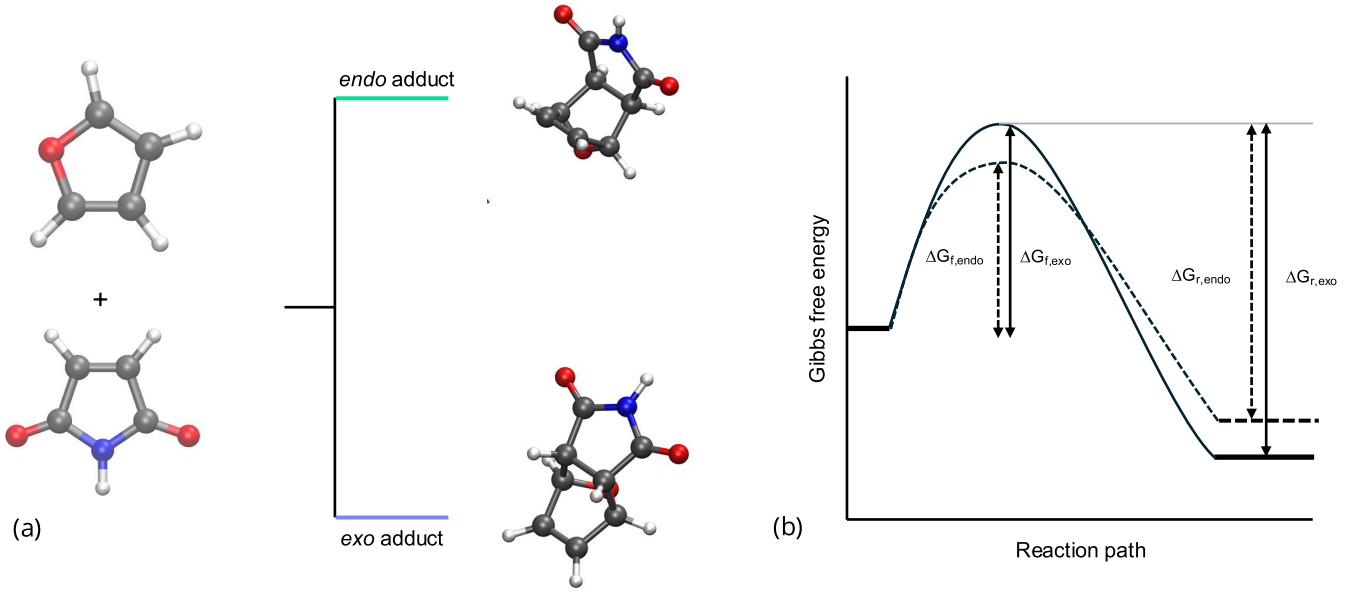


**Figure 1.** Schematic representation of the different stereochemical adducts of the furan-maleimide reaction (a) and (b) the resulting reaction paths in Gibbs free energy.

Diels–Alder reactions can form an *endo* or *exo* adduct, defined by the overlap of the functional groups on the molecules. For the cycloaddition between furan and maleimide, the *endo* adduct is formed when the carbonyl groups of the maleimide are placed toward the $\pi$ bonds of furan, while in the *exo* adduct, the carbonyl groups are turned away from furan's $\pi$ bonds. For many DA reactions, the *endo* adduct is kinetically favored, while the *exo* adduct is thermodynamically favored, as illustrated in Figure 1.

This study focuses on the furan-maleimide reaction, as it is the most widely studied reversible cross-link in CANs making it easier to benchmark our molecular dynamics (MD) simulations. Cuvellier et al. showed the importance of involving *endo* and *exo* selectivity for the furan-maleimide reaction, as the authors found that the *endo* adduct is formed first and then gradually decomposes as the system forms the more stable *exo* adduct upon curing.[14,15] Adding functional groups, and by extension polymer chains, can disrupt this preference, as well as the overall kinetics considering both reactions.[19−21] To understand the self-healing mechanism, it is therefore crucial to look at a larger system.

Empirical force field-based molecular dynamics (MD) can help us to attain this goal. However, as the making and breaking of bonds play crucial roles in the self-healing mechanism, reactive MD is required. The ReaxFF reactive force field method has already been very successful in predicting the cross-linking of epoxy-amine polymer networks.[22,23] ReaxFF MD simulations can not only provide insights into the mechanism behind the reaction but can also be used to predict macroscopic properties such as a glass transition temperature or Young's modulus using simulated heating and tensile tests.[24,25]

It is important to note that the curing and self-healing of these networks can take up to several hours, even at elevated temperatures, while ReaxFF molecular dynamics simulations typically cover only nanoseconds of time. Therefore, an acceleration technique is required for the ReaxFF simulations. As specific bonds must be targeted during this acceleration, the bond boost method as developed by Miron and Fichthorn can be applied to study reactions within reasonable timeframes.[26] This method has been adopted by Vashisth et al. to study the cross-linking in epoxy-amine systems, a case which is relatively similar to ours.[24,27] In this method, the distance and orientation of the atoms that participate in the reaction are used to find the onset to add additional energy to the system, which stretches or compresses bonds to cross the energy barrier of the reaction.

In this work, the bond boost method will be used to study the furan-maleimide retro DA reaction, as the difference between the energy barriers of the different stereochemistries is much larger for the backward reaction (3 kcal/mol) compared to the forward reaction (<1 kcal/mol). The ReaxFF force field will be trained to reproduce the forward and retro DA activation energies obtained at the density functional theory level. First, this force field, in combination with the bond boost method, will be used to study the selectivity of the gas-phase furan-maleimide retro DA reaction. Second, the effect of the polymer backbone and an increase in temperature will be evaluated as well as the bond boost influence on *exo*/*endo* selectivity. This proof of concept will serve as the basis for further studies, where a combined forward and retro DA reaction will be studied.

## METHODS

The furan and *N*-methylmaleimide Diels–Alder reactions were first studied using density functional theory (DFT) in the gas phase. The M06-2X[28] functional in combination with Grimme D3[29,30] dispersion and the cc-pVDZ[31] basis set was used to carry out the geometry optimizations and vibrational frequency analyses, as implemented in the Gaussian 16[31] software. This functional performs excellent for forward DA activation energies giving an error of 1−1.5 kcal/mol on average when combined with a double-$\zeta$ basis set[32] and for the energetics of pericyclic reactions in general.[33]

Every transition state structure was characterized by a single imaginary frequency, after which an intrinsic reaction coordinate (IRC) calculation was performed to study the reaction path on the potential energy surface (PES). Reactant complexes and products were optimized at the same level of theory. The Eyring–Polanyi equation was used to approximate the reaction rate constants at 300 K and obtain estimated *endo*/*exo* ratios:


https://doi.org/10.1021/acs.jpca.4c05470
J. Phys. Chem. A 2024, 128, 10431−10439

$$\frac{endo}{exo} = \frac{e^{-\Delta G_{act,endo}/RT}/(e^{-\Delta G_{act,endo}/RT} + e^{-\Delta G_{act,exo}/RT})}{1 - e^{-\Delta G_{act,endo}/RT}/(e^{-\Delta G_{act,endo}/RT} + e^{-\Delta G_{act,exo}/RT})} \quad (1)$$

ReaxFF is a method for performing reactive molecular dynamics simulations, where a bond order is used to define interactions between atoms. Bond formation and dissociation can be analyzed using this method, as the bond order defines a nonbonded, single, double, or triple bonded state. The total interaction energy in ReaxFF simulations depends on many energy contributions (eq 2).[34,35]

$$E_{system} = E_{bond} + E_{over} + E_{under} + E_{val} + E_{tors} + E_{vdW} + E_{Coulomb} + E_{lp} + E_{H\text{-}bond} + E_{rest} \quad (2)$$

In this equation, the energy of the system ($E_{system}$) is defined by the bond-order dependent terms such as the bond energy ($E_{bond}$), the overcoordination ($E_{coord}$), undercoordination ($E_{under}$), and hydrogen-bond interactions ($E_{H\text{-}bond}$) as well as energy penalty terms such as the torsion energy ($E_{tor}$), valence angle energy ($E_{val}$), and lone pair energy ($E_{lp}$). The van der Waals ($E_{vdW}$) and Coulomb ($E_{coulomb}$) energies are contributions that account for the nonbonded interactions. ReaxFF has been successfully used to simulate several processes such as thermal decomposition of polymers and the cross-linking of polymers.[23,36]

We used ReaxFF to optimize the geometry of several simulation boxes containing 40 *endo* and *exo* products and later for a similar simulation of 10 products containing the polymer backbone. MD simulations on these boxes were accelerated using the bond boost method. When the distances of the C atoms that participate in the bond formation are within predefined limits, an additional potential (restrain energy or $E_{rest}$ in eq 3) is added for a duration of 5000 steps—as discussed in the Results and Discussion section. The additional potential was varied through the $F_1$ force parameter, resulting in a change in the number of "successful events." The number of successful events corresponds to the number of product molecules that were decomposed into their respective reactants.[23]

$$E_{ij}^{rest} = F_1[1 - e^{F_2(R_{ij}-R_0)^2}] \quad (3)$$

In this equation, $F_1$ and $F_2$ are force parameters that can be used to fine-tune and benchmark the method, $R_{ij}$ is the current distance between atom $i$ and atom $j$, and $R_0$ is the targeted bond distance.

## RESULTS AND DISCUSSION

**Training the Force Field/Comparing to QM Data.** The initial ReaxFF force field was based on the force field from Kowalik et al. 2019,[37] and was retrained against quantum chemical data. Using M06-2X-D3/cc-pVDZ, we computed (1) the forward and retro activation barrier as well as the reaction energy (Table 1) and (2) the geometries of the studied molecules along the full reaction path. Subsequently, the force field was trained to reproduce these barriers. A comparison between the energy profiles as computed by DFT and ReaxFF using the retrained force field is shown in Figure 2.

**Table 1. Forward and Reverse Energy Barriers and Reaction Energies Based on Electronic Energies for the PESs in Figure 2**

| stoichiometry | forward activation barrier (kcal/mol) | reverse activation barrier (kcal/mol) | reaction energy (kcal/mol) |
|---|---|---|---|
| Values Computed Using DFT | | | |
| *endo* | 18.9 | 28.9 | −10.0 |
| *exo* | 19.5 | 31.1 | −11.6 |
| Values Computed Using PES in ReaxFF | | | |
| *endo* | 18.9 | 28.1 | −9.3 |
| *exo* | 19.1 | 30.8 | −11.7 |

The force field clearly approximates the DFT energies well, as differences in energy are on average 0.4 kcal/mol, with only the retro reaction barrier and the reaction energy of the *endo* reaction showing slightly larger deviations (0.8 and 0.7 kcal/mol). From the difference between the *endo* and *exo* adduct decomposition barriers, 2.2 kcal/mol for the DFT calculations and 2.7 kcal/mol for ReaxFF, the *endo*/*exo* ratio can be estimated by using the Eyring−Polanyi equation. Note that these differences are in line with earlier experimentally derived retro barriers for the furan-maleimide system as part of CANs (2.51 kcal/mol).[38] The expected ratio for the *endo* and *exo* reaction rate for bond breaking in the adduct at 298.15K using DFT is equal to 41, while the ratio for ReaxFF is expected to be 95, with the experimentally measured ratio of 69 nicely in between. Note, again, that a factor of 2 corresponds to a difference of merely 0.5 kcal/mol, so well within the chemical accuracy. This ratio will be used to verify the validity of the ReaxFF simulations, as it can be calculated from the actual concentrations of reactants and adducts in the reactive MD simulations. In a later stage, this ratio could be used to compare the simulation results to the experimental findings.

**Reverse DA Reaction: Decomposing *Endo* and *Exo* Adducts.** The bond boost method was applied to the furan/*N*-methylmaleimide system to decompose *endo* and *exo* adducts into their respective reactants. The targeted atoms are the four C atoms involved in the formation of new bonds during the (forward) Diels−Alder reaction, as shown in Figure 3, together with their possible estimated distance ranges and target distances, as used in the tracking.in file. The target distance for the bond boost was set to 3.0 Å, as this is the distance for which the reaction path is the steepest toward the reagents. This distance therefore ensures conversion of the product into separate reactants. The actual cutoff for measuring bond breakage is set at a bond order of 0.3, which corresponds to a distance of 2.45 Å, making 3.0 Å a good target. The $F_2$ force constant was kept at 0.25, as preliminary tests showed that this resulted in a system where the bond boosts were most sensitive to changing the $F_1$ parameter. The $F_1$ force constant was varied between 90 and 130 and the resulting concentrations of *endo* and *exo* reagents were evaluated. Figure S1 shows that having an $F_1$ factor higher than 130 is not useful, as all bond boosts are successful, leading to a total lack of stereoselectivity. The simulation boxes contained 40 *endo* product molecules and 40 *exo* product molecules, respectively.

Figure 4 shows the result of a simulation when the $F_1$ parameter is varied from 90 to 130. The accommodating snapshots show *endo* and *exo* products before and after a successful bond boost. The snapshot gives an idea of the density of the simulation box and the increased distance between the separated molecules after the entire simulation. Clearly, the *endo* product decomposes more easily than the *exo* product, which is in line with the reverse barrier found using both DFT and ReaxFF. Naturally, an increasing $F_1$ factor leads to a higher added potential during the bond boost and should, therefore, result in more successful bond boost attempts. This increase in


https://doi.org/10.1021/acs.jpca.4c05470
J. Phys. Chem. A 2024, 128, 10431−10439

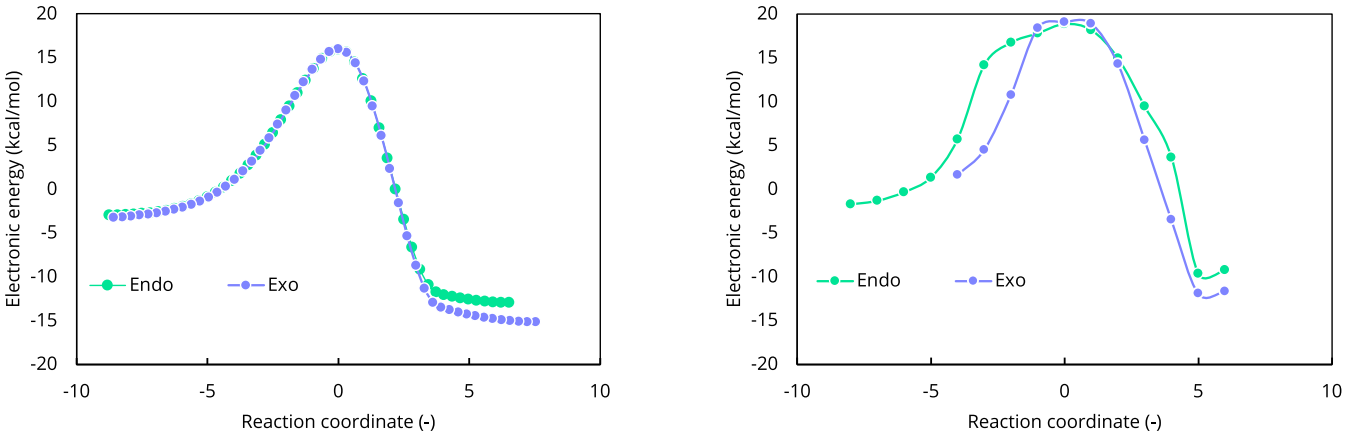


**Figure 2.** Energy profile on the potential energy surface (PES) for the endo and exo reactions between furan and *N*-methylmaleimide referenced to their separate reactants using (left) density functional theory and (right) ReaxFF. Forward and reverse energy barriers as well as reaction energies based on electronic energies are given in the adjoined table.

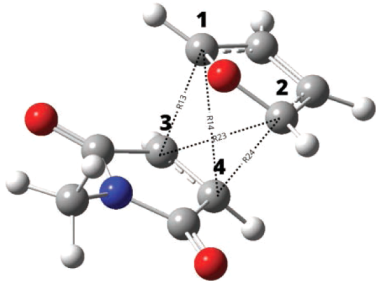


| Atoms | MINdist | MAXdist | Targetdist | F1 | F2 |
|---|---|---|---|---|---|
| C1-C3 | 1.3 | 2.7 | 3.0 | * | 0.25 |
| C1-C4 | 1.3 | 2.7 | 3.0 | * | 0.25 |
| C2-C3 | 1.3 | 2.7 | 3.0 | * | 0.25 |
| C2-C4 | 1.3 | 2.7 | 3.0 | * | 0.25 |

***** F1 force constant will be varied throughout the tests

**Figure 3.** Transition state structure of the exo adduct, indicating the atom couples that participate in the bond boost and their interatomic distances (dependent on *endo* or *exo*), being minimal distance (MINdist), maximal distance (MAXdist), and target distance (Targetdist), given in Å.

the number of successful attempts, however, is not the same for *endo* and *exo* adducts. For large values of $F_1$, we expect it to lead to a decrease in stereoselectivity (Table 2).

The simulations were run for 2,800,000 steps, or a duration of 700 ps, and repeated three times, resulting in 96 CPU hours for each simulation. The results of the separate trials are shown in Table 3. The different runs for a given parameter setting yield (slightly) different numbers of successful *endo* and *exo* retro DA reactions, as for each run the starting geometry was changed. The ratio between the number of dissociated *endo* and *exo* adducts (here defined as *endo*/*exo*) was determined at different points during the simulation, being 25, 50, and 75% decomposition of the 40 *endo* products used in the simulation. The highest ratio that was found was 20 for an $F_1$ factor of 95. When the $F_1$ factor equals 90, no *exo* reactions were observed throughout the simulation for geometry 2, which made that the *endo*/*exo* ratio could not be determined. As $F_1$ increases, the selectivity is gradually reduced until there is no difference between *endo* and *exo* adducts (*endo*/*exo* ratio equal to 1 for $F_1$ = 130).

Figure 5 plots the $F_1$ factor against the *endo*/*exo* ratio for the second simulation, indicating an exponential relationship. The error bars show a large variation in the ratios for small $F_1$ values, which is to be expected, as the number of successful attempts is then very low. For an $F_1$ value of 95, for example, the number of successful attempts for the *exo* system is as low as one, which means that an additional successful attempt can lead to a 50% reduction in the *endo*/*exo* ratio. Despite these larger variations in *endo*/*exo* ratios, the plot demonstrates that we can successfully tune the system to reflect measurable properties by using the bond boost method. The exponential nature of this curve reflects the Arrhenius relations that govern the activation barriers, which are themselves related to the Maxwell-Botzmann velocity profiles. The latter ones are Gaussians, decaying exponentially. Similar plots for the other simulations are shown in Figure SI.1−3.

**Effect of Polymer Side Chain.** The power of these MD simulations lies in the possibility of simulating what is happening inside a polymer network. To this end, the side chains used in a three-dimensional (3D) self-healing polymer network were added to the furan-maleimide moieties and their effect on the *endo*/*exo* ratio was studied. First, the system was optimized to obtain a realistic starting geometry. The $F_1$-factor was fixed at 95, as this turned out to be the optimal value for this system in the previous results. The simulation was performed for a set of 10 *endo* or *exo* products, containing side chains as illustrated in Figure 6. This polymer backbone was based on CANs made by Mangialetto et al.[13] To form a cross-linked network, one DA component should be at least trifunctional. However, since we do not yet focus on the forward barrier, it is difficult to construct such a full network. Therefore, we decided to approximate the network by selecting 10 furan-maleimide products containing chains closely resembling chains as side groups but without intermolecular connections to other DA adducts present in a network. Nonetheless, the chemical composition and bulkiness are rather similar, which allows us to make a good first estimation of the effect of the polymer surrounding on the DA reaction.

The simulated time was 100 ps instead of 700 ps, as the larger number of atoms requires a larger CPU time. Figure 7 shows the evolution of the number of FM products over time using the


https://doi.org/10.1021/acs.jpca.4c05470
J. Phys. Chem. A 2024, 128, 10431−10439

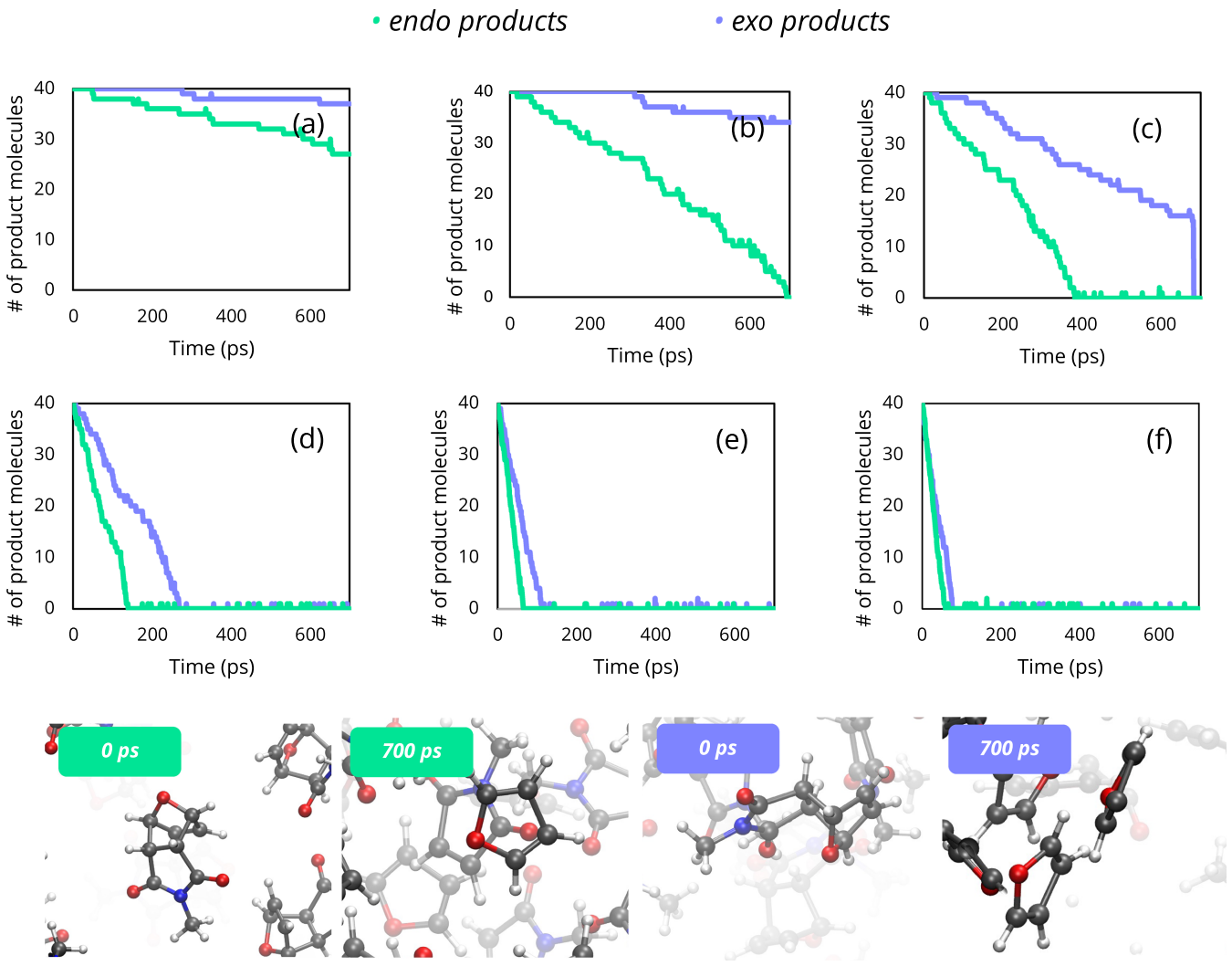


**Figure 4.** Number of products over time for simulation 1, while varying the $F_1$ force constant from (a) 90, (b) 95, (c) 100, (d) 110, and (e) 120 to (f) 130. Green refers to the *endo* adducts, whereas blue indicates exo adducts. The used box size is 50 Å × 50 Å × 50 Å, 298 K. We used a Berendsen thermostat, a canonical ensemble and a damping constant of 100 fs. The snapshots show a random *endo* and *exo* product that underwent a successful bond boost at the beginning and end of the simulation.

**Table 2. *Endo*/*Exo* Ratios for Different Simulations and at Different Degrees of *Endo* Conversion for a Range of $F_1$ Force Factors**

| % *endo* decomposed | $F_1$ = 90 | $F_1$ = 95 | $F_1$ = 100 | $F_1$ = 110 | $F_1$ = 120 | $F_1$ = 130 |
|---|---|---|---|---|---|---|
| | | | Simulation 1 | | | |
| 25 | 5 | | 10 | 2 | 2 | 1 |
| 50 | | 7 | 3 | 3 | 2 | 1 |
| 75 | | 6 | 3 | 2 | 2 | 1 |
| | | | Simulation 2 | | | |
| 25 | | 10 | 5 | 2 | 1 | 1 |
| 50 | | 7 | 4 | 2 | 2 | 1 |
| 75 | | 6 | 4 | 2 | 1 | 1 |
| | | | Simulation 3 | | | |
| 25 | 10 | 10 | | 5 | 2 | 1 |
| 50 | | 20 | 20 | 2 | 2 | 1 |
| 75 | | 15 | 4 | 2 | 2 | 1 |

bond boost method and an $F_1$ force factor equal to 95 for the substituted system compared to the unsubstituted system. The snapshots show the preferential breaking of an exemplary endo product, before and after a bond boost took place. The stereoselectivity is clearly lower than that of the unsubstituted case. In previous work,[12] we studied similar substituted systems both experimentally and computationally using DFT. While the Gibbs free energy barrier of the retro DA reaction of the unsubstituted furan-maleimide reaction is equal to 25.2 and 27.5 kcal/mol for the *endo* and *exo* reaction, respectively, the barriers for the substituted reaction are 25.6 and 26.8 kcal/mol. The difference in retro activation energy is therefore 1.3 kcal/mol for



https://doi.org/10.1021/acs.jpca.4c05470
J. Phys. Chem. A 2024, 128, 10431−10439

**Table 3. *Endo*/*Exo* Ratio for the Simulation of Furan-Maleimide Products Using $F_1$ = 95 for Different Temperatures and Different Degrees of Endo Decomposition**

| | *endo*/*exo* ratio for $F_1$ = 95 | |
|---|---|---|
| % endo decomposed | 300 K | 500 K |
| 25 | | 5 |
| 50 | 7 | 3 |
| 75 | 6 | 3 |

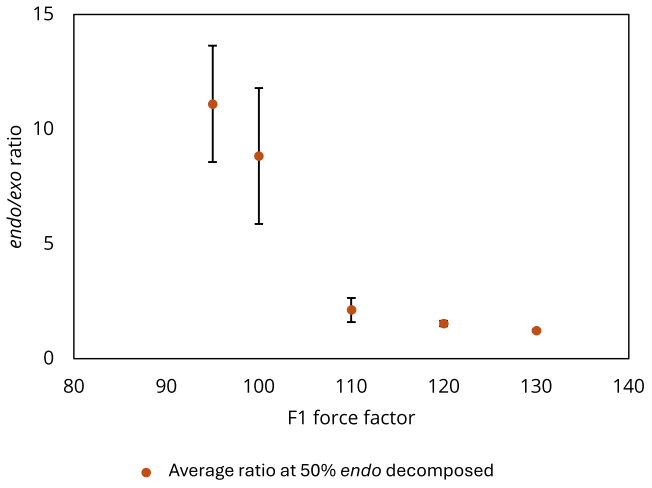


**Figure 5.** Average endo/exo ratio for several $F_1$ force factors obtained during the simulations and their respective error bars for simulations 1, 2, and 3.

the substituted case, compared to 2.3 kcal/mol for the unsubstituted case. Clearly, ReaxFF reflects this smaller difference in energy barrier, as the number of successful events is almost equal for *endo* and *exo* reactions. The higher barrier for the *exo* reaction in the unsubstituted case leads to no successful events, while the lower barrier in the substituted case leads to four successful bond boosts within the first 70 ps of the simulation.

The fact that it is possible to add a polymer backbone without reparametrizing will be mostly interesting in follow-up studies, where a forward DA reaction will be studied. This way, a unit cell that represents the macroscopic structure can be constructed, allowing for simulated heating and tensile tests on the formed polymer. This will allow one to relate the healing characteristic to the macroscopic properties and for a design support of self-healing and recyclable polymers.

**Simulations at a Higher Temperature.** Increasing the temperature leads to an increase in available energy in the system, which allows for the molecules to overcome the activation barriers when going more easily from the formed product to the reactants. In Figure 8, two cases are shown for the unsubstituted adducts, at a temperature equal to 300 and 500 K. The plots clearly show that an increase in temperature leads to a larger number of successful bond boost attempts and a lower stereoselectivity, as the *endo*/*exo* ratio lowers from 7 to 3 at a 50% decomposition of the *endo* adducts (Table 3). This shows that ReaxFF can predict temperature effects, which is very important since the studied reactions are thermoreversible.

## CONCLUSIONS AND FUTURE WORK

ReaxFF was used to simulate successfully the retro Diels–Alder reaction between furan and *N*-methylmaleimide. It allowed us to evaluate the *endo*/*exo* ratio and concentrations of remaining adducts over time and therefore to evaluate the kinetics of the reaction. Furthermore, the effect of adding a polymer backbone to these components was scrutinized, as well as the effect of temperature on the relative kinetics and stereoselectivity. It was shown that the $F_1$-force factor within the bond boost method showed the best balance between speed of the simulation and the stereoselectivity when it was equal to 95. This is a very important first step toward simulating reversible cross-links in polymer networks and thus toward the development of future sustainable materials. It opens pathways to varying the Diels–Alder components acting as linkers in the network, and evaluating the effects they have on the kinetics of the system and its self-healing capacities, something which is sometimes difficult to study using conventional experimental methods. Given the possibility to perform simulated tensile and heating tests within ReaxFF, macroscopic properties of such networks could also be studied using reactive molecular dynamics. However, to study a full network, the forward reaction must also be simulated and benchmarked against experimental results in future studies.

## ASSOCIATED CONTENT

### Supporting Information

The Supporting Information is available free of charge at https://pubs.acs.org/doi/10.1021/acs.jpca.4c05470.

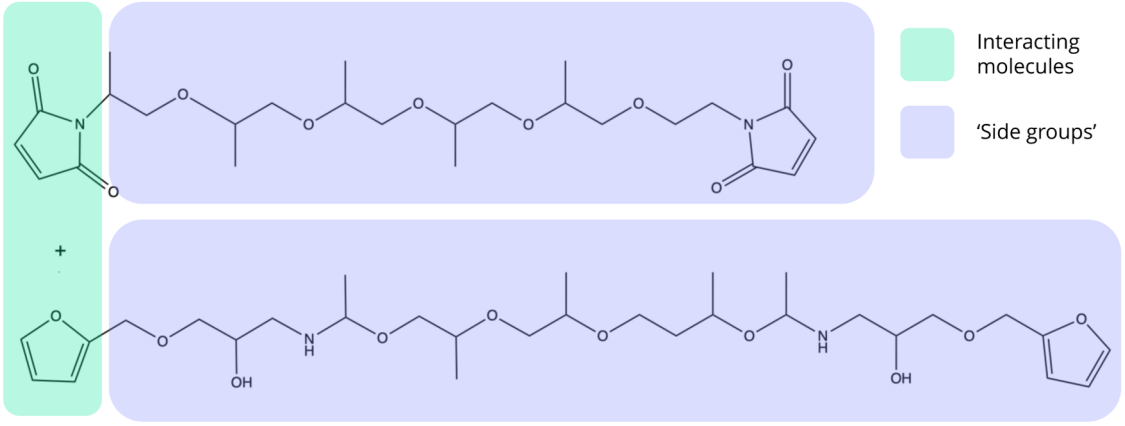


**Figure 6.** Furan and maleimide, functionalized similarly to actual systems within self-healing polymer networks.



https://doi.org/10.1021/acs.jpca.4c05470
J. Phys. Chem. A 2024, 128, 10431−10439

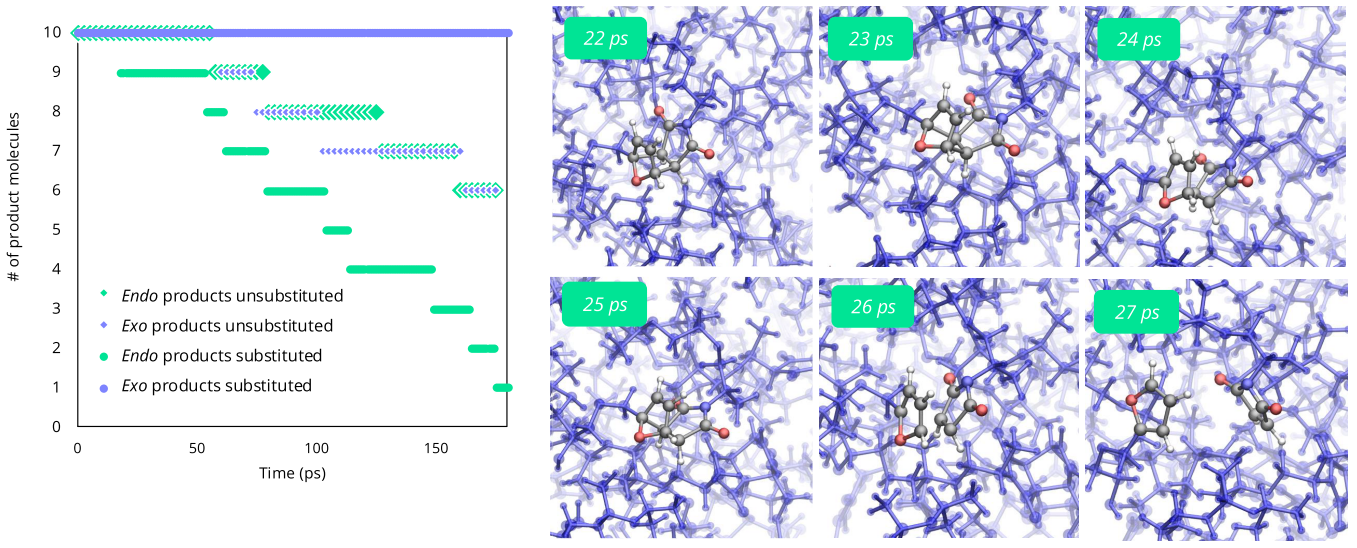


**Figure 7.** Number of products over time for simulation 1 of the unsubstituted system and for the simulation of the unsubstituted system for $F_1$ is equal to 95. The used box size is 50 Å × 50 Å × 50 Å, 298 K, a Berendsen thermostat, a canonical ensemble, and a damping constant of 100 fs. The snapshots show an endo product right before and after a successful bond boost.

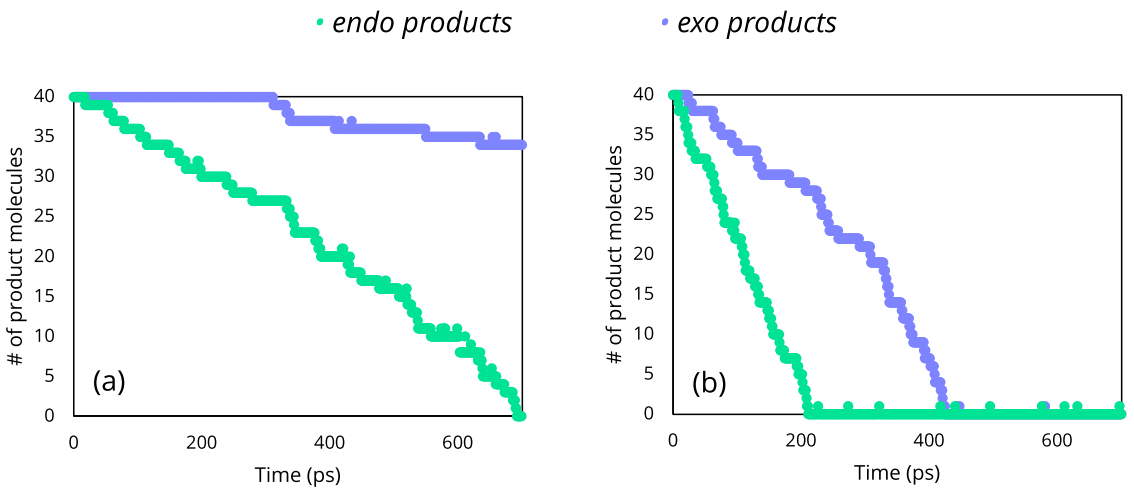


**Figure 8.** Number of products over time for of the system at (a) 300 K and (b) 500 K for $F_1$ equal to 95. The used box size is 50 Å × 50 Å × 50 Å, 298 K, a Berendsen thermostat, a canonical ensemble and a damping constant of 100 fs.

Trained force field, the system coordinates of the transition states for furan-*N*-methylmaleimide and the tracking.in file, as well as simulations for $F_1$ = 150 and 200 and simulations with different starting geometries (PDF)

## AUTHOR INFORMATION


### Corresponding Author

**A. C. T. van Duin** − *Department of Mechanical Engineering, Pennsylvania State University (PSU), University Park, Pennsylvania 16802, United States;* orcid.org/0000-0002-3478-4945; Email: acv13@psu.edu

### Authors

**L. Vermeersch** − *Algemene Chemie & Physical Chemistry and Polymer Science, Vrije Universiteit Brussel, 1050 Brussel, Belgium;* orcid.org/0000-0001-6601-9087

**T. Wang** − *Department of Mechanical Engineering, Pennsylvania State University (PSU), University Park, Pennsylvania 16802, United States*

**N. Van den Brande** − *Physical Chemistry and Polymer Science, Vrije Universiteit Brussel, 1050 Brussel, Belgium*

**F. De Vleeschouwer** − *Algemene Chemie, Vrije Universiteit Brussel, 1050 Brussel, Belgium;* orcid.org/0000-0003-0563-1509

Complete contact information is available at: https://pubs.acs.org/10.1021/acs.jpca.4c05470


### Notes

The authors declare no competing financial interest.

## ACKNOWLEDGMENTS

L.V. thanks the Fund for Scientific Research-Flanders (FWO-1164223N) for financial support. The resources and services used in this work were provided by the VSC (Flemish Supercomputer Center), funded by the Research Foundation—Flanders (FWO) and the Flemish Government. T.W. and A.C.T.v.D. acknowledge additional support from the National Science Foundation under DMR-2011839. F.D.V. wishes to

thank the VUB for the Strategic Research Program awarded to the ALGC research group.

## REFERENCES

(1) Plastic waste and recycling in the EU: facts and figures.
(2) Costa Cornellà, A.; Tabrizian, S. K.; Ferrentino, P.; Roels, E.; Terryn, S.; Vanderborght, B.; Van Assche, G.; Brancart, J. Self-Healing, Recyclable, and Degradable Castor Oil-Based Elastomers for Sustainable Soft Robotics. *ACS Sustainable Chem. Eng.* **2023**, *11* (8), 3437−3450.
(3) Guo, Y.; Zhong, J.; Zhao, P.; Xu, D.; Yue, G.; Shuai, M. Self-Healing Polymers Based on Reversible Covalent Bond. *Polym. Mater. Sci. Eng.* **2016**, *32* (12), 151−155.
(4) Scheltjens, G.; Diaz, M. M.; Brancart, J.; Van Assche, G.; Van Mele, B. In *A Self-Healing Polymer Network Based on Reversible Covalent Bonding*, 8th Asian-Australasian Conference on Composite Materials 2012, ACCM 2012—Composites: Enabling Tomorrow's Industry, 2012; pp 1318−1323.
(5) Araya-Hermosilla, R.; Lima, G. M. R.; Raffa, P.; Fortunato, G.; Pucci, A.; Flores, M. E.; Moreno-Villoslada, I.; Broekhuis, A. A.; Picchioni, F. Intrinsic Self-Healing Thermoset through Covalent and Hydrogen Bonding Interactions. *Eur. Polym. J.* **2016**, *81*, 186−197.
(6) Terryn, S.; Langenbach, J.; Roels, E.; Brancart, J.; Bakkali-Hassani, C.; Poutrel, Q. A.; Georgopoulou, A.; George Thuruthel, T.; Safaei, A.; Ferrentino, P.; et al. A Review on Self-Healing Polymers for Soft Robotics. *Mater. Today* **2021**, *1*, 187−205, DOI: 10.1016/j.mattod.2021.01.009.
(7) Reutenauer, P.; Buhler, E.; Boul, P. J.; Candau, S. J.; Lehn, J. M. Room Temperature Dynamic Polymers Based on Diels-Alder Chemistry. *Chem. - Eur. J.* **2009**, *15* (8), 1893−1900.
(8) Briou, B.; Améduri, B.; Boutevin, B. Trends in the Diels-Alder Reaction in Polymer Chemistry. *Chem. Soc. Rev.* **2021**, *50* (19), 11055−11097.
(9) Diaz, M. M.; Van Assche, G.; Maurer, F. H. J.; Van Mele, B. Thermophysical Characterization of a Reversible Dynamic Polymer Network Based on Kinetics and Equilibrium of an Amorphous Furan-Maleimide Diels-Alder Cycloaddition. *Polymer* **2017**, *120*, 176−188.
(10) Wei, Z.; Yang, J. H.; Du, X. J.; Xu, F.; Zrinyi, M.; Osada, Y.; Li, F.; Chen, Y. M. Dextran-Based Self-Healing Hydrogels Formed by Reversible Diels-Alder Reaction under Physiological Conditions. *Macromol. Rapid Commun.* **2013**, *34* (18), 1464−1470.
(11) Ehrhardt, D.; Mangialetto, J.; Van Durme, K.; Van Mele, B.; Van Den Brande, N. From Slow to Fast Self-Healing at Ambient Temperature of High-Modulus Reversible Poly(Methacrylate) Networks. Single- And Dual-Dynamics and the Effect of Phase Separation. *Macromolecules* **2021**, *54* (21), 9960−9977.
(12) Mangialetto, J.; Kiano, G.; Vermeersch, L.; Van Mele, B.; Van Den Brande, N.; De Vleeschouwer, F. Hydrogen-Bond-Assisted Diels−Alder Kinetics or Self-Healing in Reversible Polymer Networks? A Combined Experimental and Theoretical Study. *Molecules* **2022**, *27*, No. 1961.
(13) Mangialetto, J.; Cuvellier, A.; Verhelle, R.; Brancart, J.; Rahier, H.; Van Assche, G.; Van Den Brande, N.; Van Mele, B. Diffusion- A Nd Mobility-Controlled Self-Healing Polymer Networks with Dynamic Covalent Bonding. *Macromolecules* **2019**, *52* (21), 8440−8452.
(14) Cuvellier, A.; Verhelle, R.; Brancart, J.; Vanderborght, B.; Van Assche, G.; Rahier, H. The Influence of Stereochemistry on the Reactivity of the Diels-Alder Cycloaddition and the Implications for Reversible Network Polymerization. *Polym. Chem.* **2019**, *10* (4), 473−485.
(15) Terryn, S.; Brancart, J.; Roels, E.; Verhelle, R.; Safaei, A.; Cuvellier, A.; Vanderborght, B.; Van Assche, G. Structure-Property Relationships of Self-Healing Polymer Networks Based on Reversible Diels-Alder Chemistry. *Macromolecules* **2022**, *55* (13), 5497−5513.
(16) Safaei, A.; Terryn, S.; Vanderborght, B.; Van Assche, G.; Brancart, J. The Influence of the Furan and Maleimide Stoichiometry on the Thermoreversible Diels−Alder Network Polymerization. *Polymers* **2021**, *13* (15), No. 2522.
(17) Diaz, M. M.; Brancart, J.; Van Assche, G.; Van Mele, B. Room-Temperature versus Heating-Mediated Healing of a Diels-Alder Crosslinked Polymer Network. *Polymer* **2018**, *153*, 453−463.
(18) Van Assche, G.; Van Hemelrijck, A.; Rahier, H.; Van Mele, B. Modulated Differential Scanning Calorimetry: Isothermal Cure and Vitrification of Thermosetting Systems. *Thermochim. Acta* **1995**, *268* (C), 121−142.
(19) Chung, Y. S.; Duerr, B. F.; Nanjappan, P.; Czarnik, A. W. Diene-Substituent Effects on the Rate. *J. Org. Chem.* **1988**, *53* (7), 1334−1336.
(20) Boutelle, R. C.; Northrop, B. H. Substituent Effects on the Reversibility of Furan-Maleimide Cycloadditions. *J. Org. Chem.* **2011**, *76* (19), 7994−8002.
(21) Khan, T. S.; Gupta, S.; Ahmad, M.; Alam, M. I.; Haider, M. A. Effect of Substituents and Promoters on the Diels-Alder Cycloaddition Reaction in the Biorenewable Synthesis of Trimellitic Acid. *RSC Adv.* **2020**, *10* (51), 30656−30670.
(22) Senftle, T. P.; Hong, S.; Islam, M. M.; Kylasa, S. B.; Zheng, Y.; Shin, Y. K.; Junkermeier, C.; Engel-Herbert, R.; Janik, M. J.; et al. The ReaxFF Reactive Force-Field: Development, Applications and Future Directions. *npj Comput. Mater.* **2016**, *2*, No. 15011, DOI: 10.1038/npjcompumats.2015.11.
(23) Vashisth, A.; Ashraf, C.; Zhang, W.; Bakis, C. E.; Van Duin, A. C. T. Accelerated ReaxFF Simulations for Describing the Reactive Cross-Linking of Polymers. *J. Phys. Chem. A* **2018**, *122* (32), 6633−6642.
(24) Vashisth, A.; Ashraf, C.; Bakis, C. E.; van Duin, A. C. T. Effect of Chemical Structure on Thermo-Mechanical Properties of Epoxy Polymers: Comparison of Accelerated ReaxFF Simulations and Experiments. *Polymer* **2018**, *158*, 354−363.
(25) Kowalik, M.; Ashraf, C.; Damirchi, B.; Akbarian, D.; Rajabpour, S.; Van Duin, A. C. T. Atomistic Scale Analysis of the Carbonization Process for C/H/O/N-Based Polymers with the ReaxFF Reactive Force Field. *J. Phys. Chem. B* **2019**, *123* (25), 5357−5367.
(26) Fichthorn, K. A.; Mubin, S. Hyperdynamics Made Simple: Accelerated Molecular Dynamics with the Bond-Boost Method. *Comput. Mater. Sci.* **2015**, *100*, 104−110.
(27) Radue, M. S.; Jensen, B. D.; Gowtham, S.; Klimek-McDonald, D. R.; King, J. A.; Odegard, G. M. Comparing the Mechanical Response of Di-, Tri-, and Tetra-Functional Resin Epoxies with Reactive Molecular Dynamics. *J. Polym. Sci., Part B: Polym. Phys.* **2018**, *56* (3), 255−264.
(28) Zhao, Y.; Truhlar, D. G. The M06 Suite of Density Functionals for Main Group Thermochemistry, Thermochemical Kinetics, Noncovalent Interactions, Excited States, and Transition Elements: Two New Functionals and Systematic Testing of Four M06-Class Functionals and 12 Other Function. *Theor. Chem. Acc.* **2008**, *120* (1−3), 215−241.
(29) Grimme, S.; Hansen, A.; Brandenburg, J. G.; Bannwarth, C. Dispersion-Corrected Mean-Field Electronic Structure Methods. *Chem. Rev.* **2016**, *116* (9), 5105−5154.
(30) Dunning, T. H. Gaussian Basis Sets for Use in Correlated Molecular Calculations. I. The Atoms Boron through Neon and Hydrogen Gaussian Basis Sets for Use in Correlated Molecular Calculations. I. The Atoms Boron through Neon and Hydrogen. *J. Phys. Chem. A* **1989**, *90*, 1007−1023.
(31) Frisch, M. J.; Trucks, G. W.; Schlegel, H. B.; Scuseria, G. E.; Robb, M. A.; Cheeseman, J. R.; Scalmani, G.; Barone, V.; Petersson, G. A.; Nakatsuji, H.;et al. *Gaussian 16*, revision C.01; Gaussian Inc: Wallingford, CT, 2016.
(32) Tang, S. Y.; Shi, J.; Guo, Q. X. Accurate Prediction of Rate Constants of Diels-Alder Reactions and Application to Design of Diels-Alder Ligation. *Org. Biomol. Chem.* **2012**, *10* (13), 2673−2682.
(33) Vermeeren, P.; Dalla Tiezza, M.; Wolf, M. E.; Lahm, M. E.; Allen, W. D.; Schaefer, H. F.; Hamlin, T. A.; Bickelhaupt, F. M. Pericyclic Reaction Benchmarks: Hierarchical Computations Targeting CCSDT-(Q)/CBS and Analysis of DFT Performance. *Phys. Chem. Chem. Phys.* **2022**, *24* (30), 18028−18042.
(34) Chenoweth, K.; Van Duin, A. C. T.; Goddard, W. A. ReaxFF Reactive Force Field for Molecular Dynamics Simulations of Hydrocarbon Oxidation. *J. Phys. Chem. A* **2008**, *112* (5), 1040−1053.


https://doi.org/10.1021/acs.jpca.4c05470
J. Phys. Chem. A 2024, 128, 10431−10439

(35) Van Duin, A. C. T.; Dasgupta, S.; Lorant, F.; Goddard, W. A. ReaxFF: A Reactive Force Field for Hydrocarbons. *J. Phys. Chem. A* **2001**, *105* (41), 9396−9409.
(36) Keten, S.; Chou, C. C.; van Duin, A. C. T.; Buehler, M. J. Tunable Nanomechanics of Protein Disulfide Bonds in Redox Microenvironments. *J. Mech. Behav. Biomed. Mater.* **2012**, *5* (1), 32−40.
(37) Kowalik, M.; Ashraf, C.; Damirchi, B.; Akbarian, D.; Rajabpour, S.; Van Duin, A. C. T. Atomistic Scale Analysis of the Carbonization Process for C/H/O/N-Based Polymers with the ReaxFF Reactive Force Field. *J. Phys. Chem. B* **2019**, *123* (25), 5357−5367.
(38) Mangialetto, J.; Verhelle, R.; Van Assche, G.; Van Den Brande, N.; Van Mele, B. Time-Temperature-Transformation, Temperature-Conversion-Transformation, and Continuous-Heating-Transformation Diagrams of Reversible Covalent Polymer Networks. *Macromolecules* **2021**, *54* (1), 412−425.



https://doi.org/10.1021/acs.jpca.4c05470
*J. Phys. Chem. A* 2024, 128, 10431−10439